

Influence of Bearing Stiffness on the Static Properties of a Planetary Gear System with Manufacturing Errors

Cheon Gill-Jeong*

*Division of Mechanical Engineering, Wonkwang University,
Iksan City, Jeon-Buk 570-749, Korea*

Robert G. Parker

*Department of Mechanical Engineering, The Ohio State University,
Columbus, OH 43220-1107, USA*

Hybrid finite element analysis was used to analyze the influence of bearing stiffness on the static properties of a planetary gear system with manufacturing errors. The effects of changes in stiffness were similar for most of the manufacturing errors. State variables were most affected by the stiffness of the planet bearings. Floating either the sun or carrier helps to equal load sharing and minimizes the critical tooth stress. The effects of a floating sun and carrier are similar, but it is not recommended that both float, because this can induce greater critical tooth stress. Planet bearing stiffness should be optimized. Both load sharing and critical tooth stress should be considered to determine optimal bearing stiffness.

Key Words : Planetary Gear, Manufacturing Error, Bearing Stiffness, Load Sharing, Gear

1. Introduction

Planetary gear systems are widely used in various power transmission applications due to their unique characteristics. Planetary gear systems have multiple gear components and a more complicated geometry than conventional parallel shaft gear systems. Consequently, shape or positioning errors involving even one element affect the behavior of the whole.

In real systems, some manufacturing errors, such as positioning or tooth thickness errors affecting a gear, are unavoidable, and they induce much more unequal load sharing than in the normal (no-error) condition (Bodas and Kahraman, 2001; Cheon and Oh, 2003; Cheon, 2003; Cheon and Parker, 2004). It is essential to pro-

vide countermeasures at the design stage to minimize these unavoidable negative effects. The designer can control state variables, such as bearing force and critical stress, by using design parameters at the design stage. Since most of the parameters related to gears are determined by the system requirements, the range of design parameters is strictly restricted. Bearing stiffness and ring gear boundary conditions are design parameters that can be handled relatively easily without regard to gear-related parameters.

Many studies have examined the effects on planet bearing load sharing of a floating sun or carrier (Hidaka and Terauchi, 1976; Kahraman and Vijayakar, 2001; Kahraman et al., 2003). These studies focused on the effect of the floating sun or carrier, and concluded that at least one central member must be allowed to float radially to distribute the total load as equally as possible among the planets. James and Harris (2002) analyzed the effect of the radial internal clearance (RIC) of the planet bearing, and planet carrier and ring gear stiffness on unequal planet load sharing. They discovered that the RIC of the sun

* Corresponding Author,

E-mail : gjcheon@wonkwang.ac.kr

TEL : +82-63-850-6686; **FAX :** +82-63-850-6691

Division of Mechanical Engineering, Wonkwang University, Iksan City, Jeon-Buk 570-749, Korea. (Manuscript Received May 4, 2004; Revised August 16, 2004)

does not eliminate unequal load sharing, while the RIC of a planet does relieve unequal load sharing. They also found that compliance of the carrier and ring gear reduced inequality in load sharing.

All previous studies of planet load sharing have restricted their analyses to systems without manufacturing errors. None have analyzed the effect of bearing stiffness on load sharing or on the critical stresses in a system with manufacturing errors, despite the fact that gear and bearing failures are the main causes of failure in planetary gear systems (Townsend, 1991).

This study characterized the effects of bearing stiffness on the static properties of a planetary gear system with manufacturing errors. The stiffness of the sun, carrier, and planet bearings was varied widely. Errors were included in the sun, ring, and planetary gears. The manufacturing errors considered in this study were tooth thickness, runout, and positioning errors, because these are the most common errors related to tolerance control in gear systems. The results might be applied to minimizing the negative effects of unavoidable manufacturing errors.

2. Computational Model

The nominal rigid-body motions of the components were determined using basic planetary gear kinematics (Cheon et al., 1999; Kahraman, 1994; Lin and Parker, 1999). The computational model calculated gear component deflections relative to the nominal motions, as well as elastic tooth deflections/stresses and bearing loads. A hybrid finite element method was used to compute two-dimensional deformations and the stresses on gear components. To avoid generating an extremely large number of elements to model the continuously moving contact zones, they were divided into two separate regions. For the contact region closest to the tooth surface (inner region), the Bousinesq solution for a point load acting on a half-space and contact forces are integrated over the tooth contact region to accurately represent relative displacements, though absolute displacements will not be accurate because of overall

tooth bending about the root. Outside the immediate vicinity of the contact zone (outer region), finite element analysis effectively models the elastic body response, including gross deflections associated with tooth bending. The two solutions were matched along the interface between the inner and outer regions. Attaching a reference frame to each individual component separately, a search was carried out over all possible surface pairings to determine which surface instances could make contact. The changing mesh stiffness and contact forces were evaluated internally at each time step as the gears rolled through the mesh. Details can be found in the references (ANSol, 2003; Cheon and Parker, 2004; Parker et al., 2000; Vijayakar, 1991).

In a planetary gear system, each gear undergoes large rotation according to kinematic relationships. The elastic deformations of the gears that superpose on the rigid body motion are small. By measuring the finite element displacement vector \mathbf{X}_{fi} for a particular gear i with respect to a reference frame that follows the rigid body motion, it is possible to represent its behavior by a linear system of differential equations (Parker et al., 2000)

$$\mathbf{M}_{ffi}\ddot{\mathbf{X}}_{fi} + \mathbf{C}_{ffi}\dot{\mathbf{X}}_{fi} + \mathbf{K}_{ffi}\mathbf{X}_{fi} = \mathbf{f}_{fi} \quad (1)$$

where \mathbf{f}_{fi} is the vector of specified external loads. Rayleigh's damping model is used in the form

$$\mathbf{C}_{ffi} = \mu\mathbf{M}_{ffi} + \eta\mathbf{K}_{ffi} \quad (2)$$

μ and η are constant Rayleigh coefficients, and are adjusted to satisfy damping properties of the material. In this study, 479 and 1.2×10^{-7} are used for μ and η , respectively.

The equations for each gear are assembled into the entire planetary gear system as

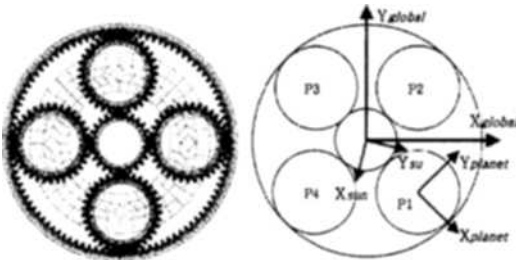
$$\mathbf{M}\ddot{\mathbf{X}} + \mathbf{C}\dot{\mathbf{X}} + \mathbf{K}\mathbf{X} = \mathbf{f} \quad (3)$$

M , C and K represent mass, damping and stiffness matrices for the system. The Newmark method was used for time integration of the equation of motion.

The system analyzed was the Army OH-58 Kiowa helicopter planetary gear. Figure 1 shows the schematics of this system, which has four

Table 1 Gear data for the OH-58 Kiowa planetary gear set

	Sun	Ring	Planet
Number of Teeth	27	99	35
Module (mm)	2.868	2.778	2.868
Outer Diameter (mm)	84.07	304.8	105.0
Root Diameter (mm)	70.55	284.1	91.54
Minor Diameter (mm)		271.8	
Bore Diameter (mm)	57.15		73.66
Face Width (mm)	25.4		
Young's Modulus (N/m ²)	207 × 10 ⁹		
Poisson's Ratio	0.3		
Density (kg/m ³)	7595		

**Fig. 1** Schematics of a four-planet gear system; the input sun gear rotates clockwise

planets, and the parameters are given in Table 1. The planets were unequally spaced at 0°, 91.4°, 180°, and 271.4°, with different mesh phasing. The outer ring gear circle is rigidly fixed with no deformation, although tooth deflection is allowed. The inner races of the sun and planets were modeled as rigid circles supported by isotropic, linear bearings. The bearings were modeled as rigid outer and inner races connected by a 3 × 3 diagonal stiffness matrix containing elements of specific magnitude for the two-dimensional translational degrees of freedom. The bearing stiffness was varied from 1 × 10⁶ N/m to 1 × 10⁹ N/m including floating condition (0 N/m). The stiffness for rotational motion was zero. The elastically deformable teeth were modeled as spurs with perfect involute shape. A constant external sun gear input torque comprised the external forcing. The nominal input torque was 1,410 N-m. The output shaft was connected to the carrier,

whose rotational deflection was constrained to zero. The number of time steps per one mesh cycle was 27.

The axis of the carrier was assumed to be the origin for the fixed reference frame (Fig. 1). Ideally, the sun and ring gear axes align with this origin. However, an assembly error can cause the centers of the sun and ring to be non-coincident with that of the carrier. In this study, positioning errors of the sun and ring gears were specified only in the positive x direction of the global coordinates. Only one of the planets (Planet 1) was assumed to have a positioning error, and the error was specified as in the radial or tangential (circumferential) direction of the carrier.

Runout error can be generated by making the axis of a gear non-coincident with the center of its pitch circle. In case of planet, only one of the planets (Planet 1) was assumed to have runout error, and the error was specified in the x direction of the planet's coordinates.

Tooth thickness error is the amount by which the circular tooth thickness in the pitch circle exceeds the nominal amount. When whole teeth of the sun or ring gear were supposed to have thickness errors, magnitudes and patterns of the bearing forces were almost similar to those of normal condition irrespective of the error size. Because sun and ring gear mesh with four planets simultaneously, the effects of thickness error cancelled each other by symmetric meshing. Hence, it was assumed that one quarter of the successive teeth on the sun and ring gears had thickness errors, to guarantee that at least one tooth with an error kept meshing with one of the four planets, and that all the teeth of one planet (Planet 1) had a thickness error.

All the positioning, runout, and thickness errors were assigned to be positive in this analysis. The error was selected as positive 25 μm.

Loads on each planet bearing F_i were compared by the load sharing (LS) of each planet as

$$LS_i = \frac{F_i}{\sum_{j=1}^4 F_j}, \quad i=1 \text{ to } 4 \quad (4)$$

Overload sharing is defined as the maximum peak

value of the load sharing over the mean average value (25%). Since the sun gear was smaller than the planet in our model, the sun gear teeth engaged much more frequently than the planet or ring gear teeth. Hence, this study investigated both of tensile and compressive principal normal stresses over the whole surface only of the sun gear. The maximum absolute values of the tensile and compressive principal stresses were traced as the maximum and minimum critical stresses. Because failure itself was not examined in this study, principal stress rather than von-Mises stress were adopted for comparison.

3. Parametric Studies

The resultant sun, carrier, and planet bearing forces as well as the planet load sharing for the normal condition are shown in Fig. 2. Due to the symmetry of the planetary gears, the sun and carrier bearing forces were much smaller than those of the planet bearings. Due to the unequal spacing, the four planets had different phasing and load magnitudes. Nevertheless, the four bearings shared the load almost equally at 25% each, and overload sharing values were small. The bearing forces fluctuated as the tooth meshes engaged.

Figure 3 shows the maximum bearing force as a function of the sun bearing stiffness in the normal condition keeping the stiffness of the other bearings at 100×10^6 N/m. The bearing forces were normalized using the values of the normal condition with stiffness in all bearings set at 100×10^6 N/m.

It is only natural that the sun bearing force increased with sun bearing stiffness, because bearing force equals the deformation times the stiffness. The carrier bearing force was slightly affected by the sun bearing's stiffness, but the effect was minimal at any specific stiffness. The planet bearing forces, load sharing, and critical stresses were barely affected by a change in the stiffness of the sun bearing. The effect of a floating sun gear was negligible in the normal condition.

Figures 4 and 5 show the maximum bearing forces, overload sharing, and critical stresses as

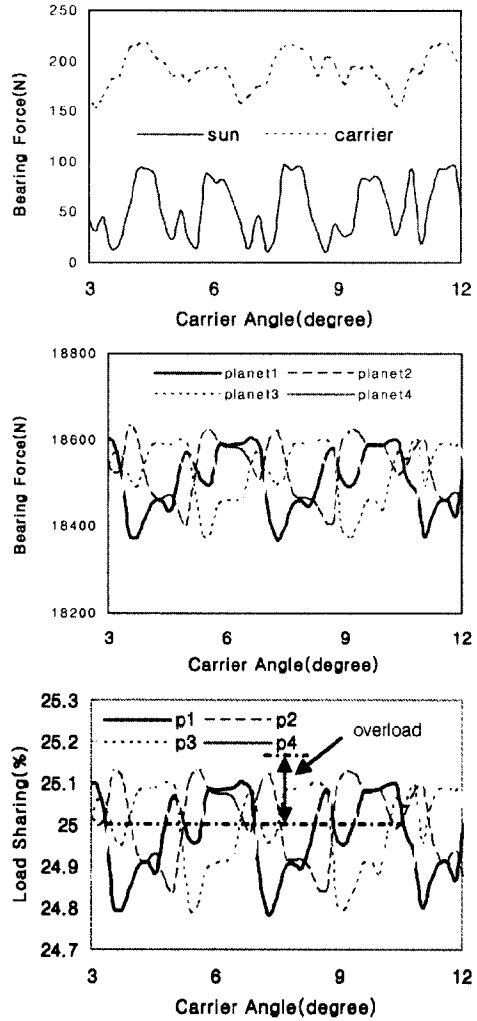


Fig. 2 Bearing forces and load sharing in the normal condition

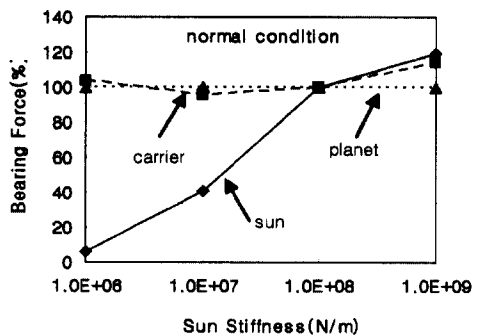


Fig. 3 Maximum bearing forces as a function of sun bearing stiffness in the normal condition

functions of sun and carrier bearing stiffness, respectively, in the sun position error condition.

Unlike the no-error condition, the carrier bearing force, planet load sharing, and critical stresses depended on the stiffness of the sun gear; values decreased with stiffness. As the stiffness decreases, the position of the sun gear can be adjusted easily to increase equal load sharing. In the normal condition, when the center of the sun gear coincides with that of the carrier, the distances between the center of the sun and the

centers of the four planets are all equal. Hence, any variation in sun and carrier gear bearing stiffness contributes little to displacements of the planets and carrier. By contrast, with an error in the position of the sun gear, the centers of the sun and four planets are not equidistant. In this case, variation in the stiffness of the sun and carrier bearings contributes greatly to the displacement of the sun gear and thereby to the distances between the centers of the sun and planets, and induces an imbalance in force between the

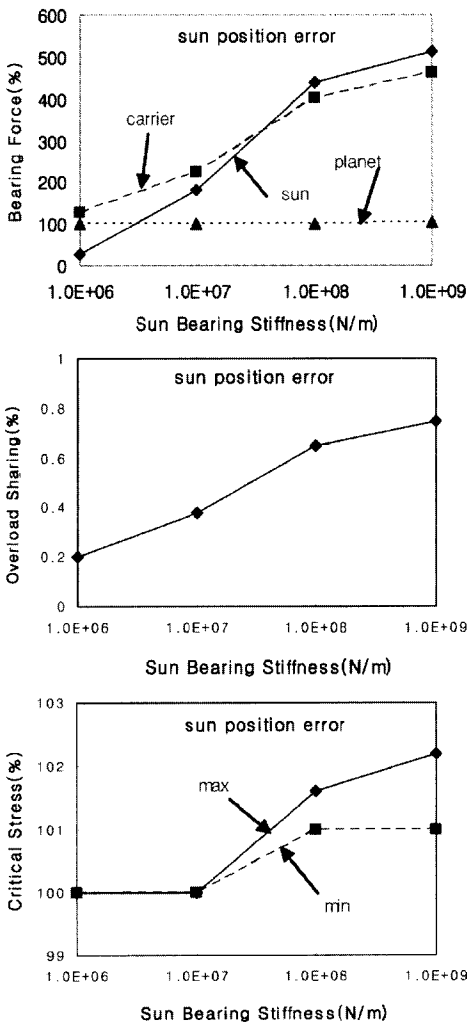


Fig. 4 Maximum bearing forces, overload sharing, and critical stresses as a function of sun bearing stiffness in the sun position error condition

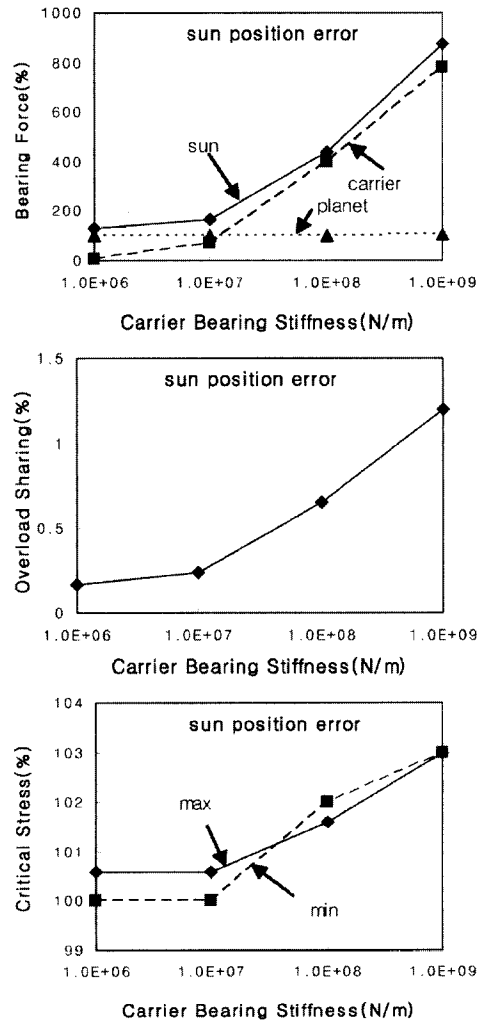


Fig. 5 Maximum bearing forces, overload sharing, and critical stresses as a function of carrier bearing stiffness in the sun position error condition

four planets. It is similar to a system with four parallel springs of different lengths.

The bearing forces at a stiffness value of 0 N/m (floating sun) were almost the same as those at 1×10^6 N/m. To decrease bearing forces, overload sharing, and critical stresses, it is equally effective to decrease the stiffness of the sun or the carrier ; either a floating sun or a floating carrier is effective for planet load sharing.

The trends in the case of sun runout error are similar to those with sun position error.

Figure 6 shows the maximum bearing forces,

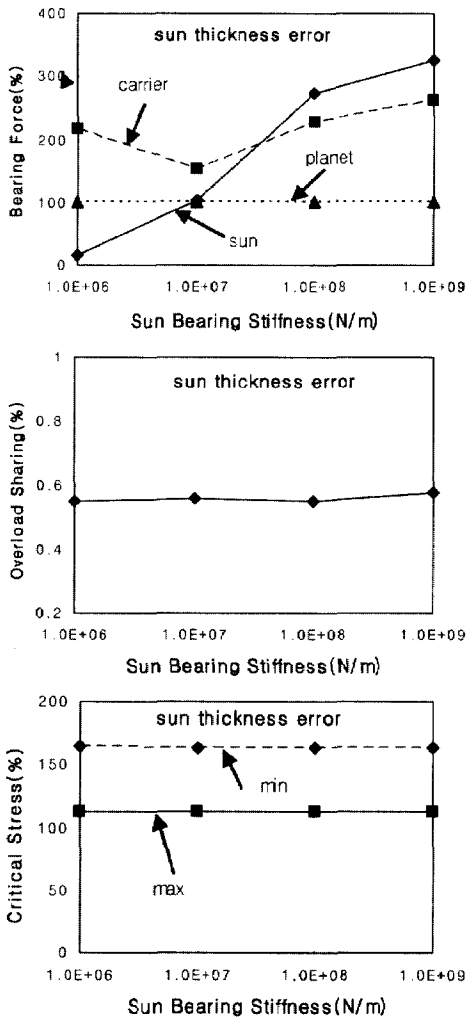


Fig. 6 Maximum bearing forces, overload sharing, and critical stresses as a function of sun bearing stiffness in the case of sun thickness error

overload sharing, and critical stresses as a function of the stiffness of the sun bearing in the sun gear tooth thickness error condition. Sun bearing force is directly related to sun bearing stiffness, but the carrier and planet bearing forces, overload sharing, and critical stresses are little affected by the stiffness of the sun bearing. Since thickness error is not a translational error, but is a rotational displacement error, thickness error in the sun gear contributes little to the translational displacement of the sun gear. Hence, load sharing and critical stress, which are sensitive to translational displacement, are little affected by the translational bearing stiffness in the case of sun gear tooth thickness error.

Figure 7 shows load sharing as a function of the carrier rotation angle in the case of planet tangential position error (Planet 1) with the stiffness of all bearings at 100×10^6 N/m. The planet with a positioning error (P1) always shares the highest load.

Figure 8 shows the state variables in the planet tangential position error condition as a function of the sun bearing stiffness. The trends are very similar to the sun position error conditions.

The effects of changes in the carrier bearing's stiffness on the bearing forces and load sharing were similar to those of variation in the stiffness of the sun bearing both in the normal condition and error conditions, because the kinematic effects of the sun and carrier on the system are similar.

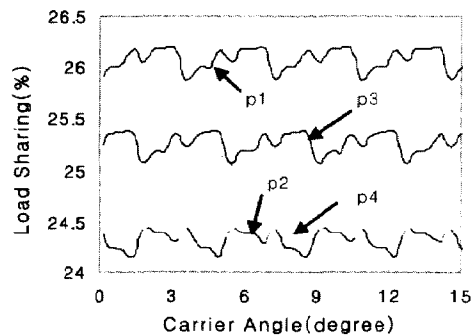


Fig. 7 Load sharing in the case of planet tangential position error : The stiffness of all bearings is 100×10^6 N/m

Figure 9 shows the various state variables as a function of planet bearing stiffness in the no-error normal condition. The sun and carrier bearing forces as well as the critical stresses increased rapidly as planet bearing stiffness decreased below a specific value. As the stiffness decreases, the deformation of the reference frame of the planets and the bearing deformation increase. This causes the trajectories of the planets to increase, and the symmetry of the tooth meshing forces around the sun and carrier to decrease.

Hence, the sun and carrier bearing forces and the critical stresses increase. The stiffness of the planet should be within a specific tolerance value to prevent the sun and carrier bearing forces from increasing rapidly. Maximum overload sharing has a minimum at a specific value. Since the planet bearing force is two orders of magnitude larger than the sun and carrier bearing forces, the bearing stiffness of the planet affects the system properties more than the stiffness of the sun and carrier bearing systems.

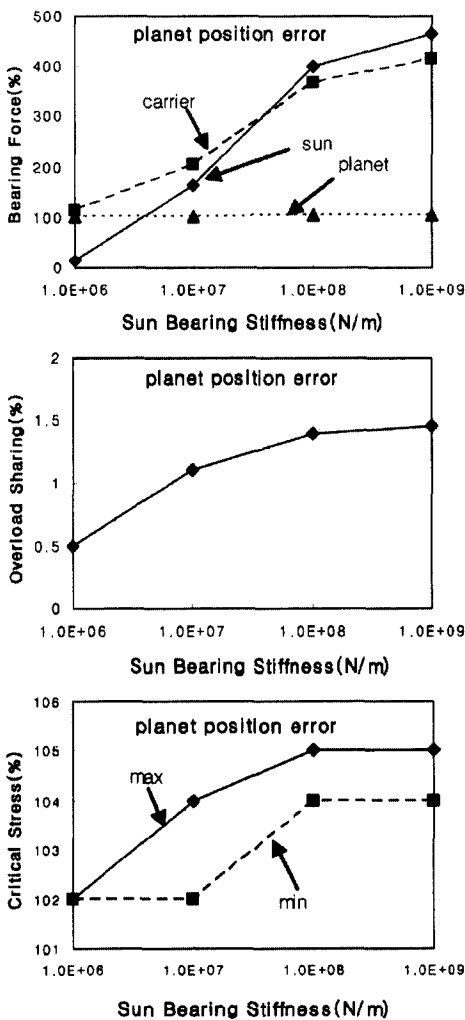


Fig. 8 Maximum bearing forces, overload sharing, and critical stress as a function of sun bearing stiffness in the case of planet tangential position error

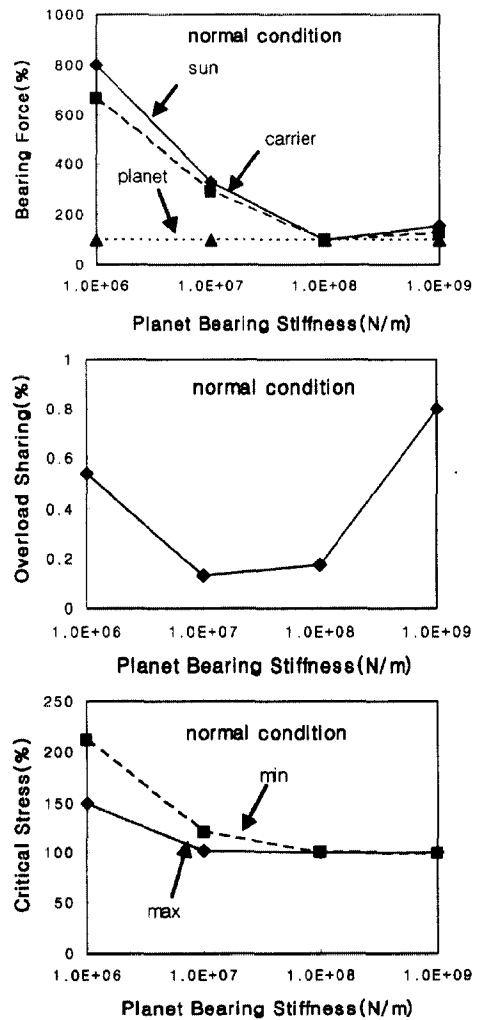


Fig. 9 Maximum bearing forces, overload sharing, and critical tooth stresses as a function of planet bearing stiffness in the normal condition

Figure 10 shows the various state variables as a function of planet bearing stiffness in the planet tangential position error condition. Unlike the cases of sun and carrier bearing stiffness, the bearing forces and critical stresses begin to increase as the stiffness falls below a specific value. When the stiffness is too high, the front planet, which leads the other planets due to phasing difference, has the highest load, because the high stiffness impedes adjustment of position to share the load. When the stiffness is too low, the planets move

far from their ideal positions, and this also contributes to increasing overload sharing. In view of the critical stresses and effect on planet load sharing, the stiffness of planet bearings should be optimized.

Since the sun and carrier are central elements surrounded by other elements that are confined to move within a limited area, low stiffness contributes to load sharing. Since the planets are not positioned centrally, low stiffness contributes more to deformation than to load sharing.

The trends in the sun position error condition as functions of planet bearing stiffness are very similar to those in the planet tangential position error conditions.

Figure 11 shows various state variables as a function of planet bearing stiffness in the sun gear tooth thickness error condition. Although sun gear tooth thickness error contributes little to the translational displacement of the sun gear center, its rotational displacement error does affect the phasing of the four planets around the sun gear. Since the tooth mesh phases of the four planets differ, the forces acting where the sun meshes with each of the planets differ. The translational displacement of the planets depends not only on the mesh force, but also on planet bearing stiffness. Hence, planet bearing stiffness affects the bearing force and load sharing of each planet more than does sun bearing stiffness.

Though it is desirable to keep the stiffness of the planet bearing as high as possible for critical stress, the stiffness should be kept at a specific value for bearing forces and load sharing. Hence, to determine the optimal value, a trade-off is necessary considering bearing forces, load sharing, and critical stresses related to bearing failure, tooth breakage, and pitting.

The effects of bearing stiffness with ring gear-related errors are similar to those of sun gear related errors.

The general effect of bearing stiffness in the case of planet runout error is very similar to that of planet tangential position error.

The general effect of different bearing stiffness in the case of planet tooth thickness error is very similar to that of sun tooth thickness error.

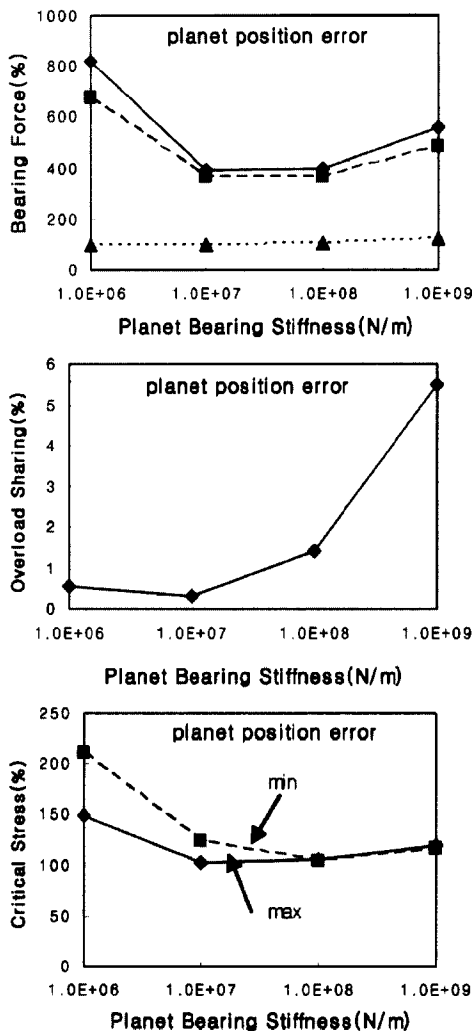


Fig. 10 Maximum bearing forces, overload sharing, and critical stress as a function of planet bearing stiffness in the case of planet tangential position error

For increasing equal load sharing, sun or carrier is usually floated. To verify most effective condition, various conditions are simulated : floating sun only, carrier only, and both of them.

Figures 12~14 show the maximum percent value of the planet bearing force as well as the maximum and minimum critical stresses for various floating conditions. The planet bearing forces are slightly lower when both the sun and carrier are floating as compared with when only one of them is floating in almost every condition.

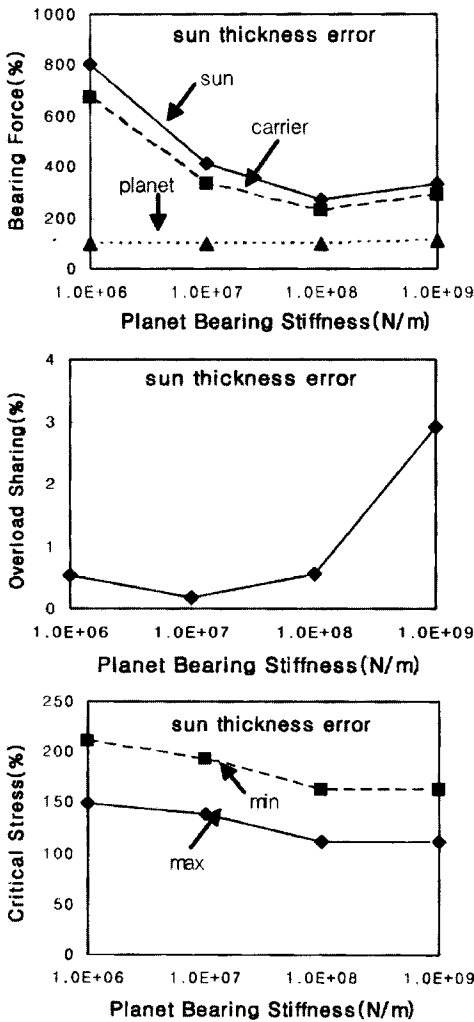


Fig. 11 Maximum bearing forces, overload sharing, and critical stress as a function of planet bearing stiffness in the sun gear tooth thickness error condition

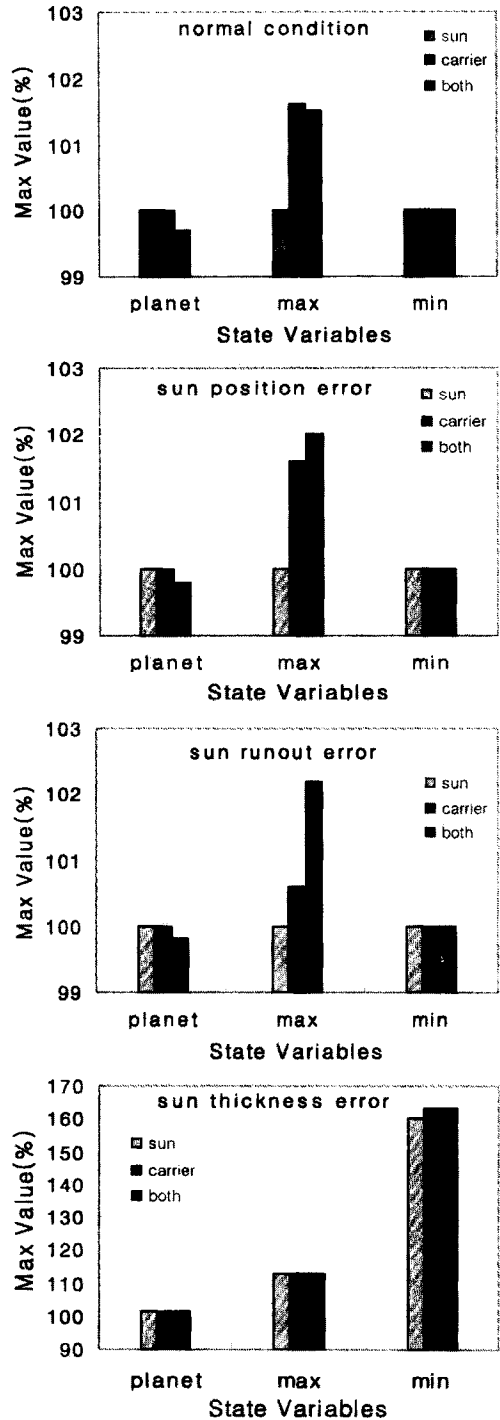


Fig. 12 Maximum percent value of planet bearing force, and maximum and minimum critical stresses as effects of a floating sun only, floating carrier only, and both, in normal and sun gear error conditions

However, floating both of the central position elements causes the maximum critical stress to be larger than when only one is floating. There does not appear to be any advantage in floating the sun only versus floating the carrier only. Considering both load sharing and critical stress, it is better to float either the sun or the carrier than to float both.

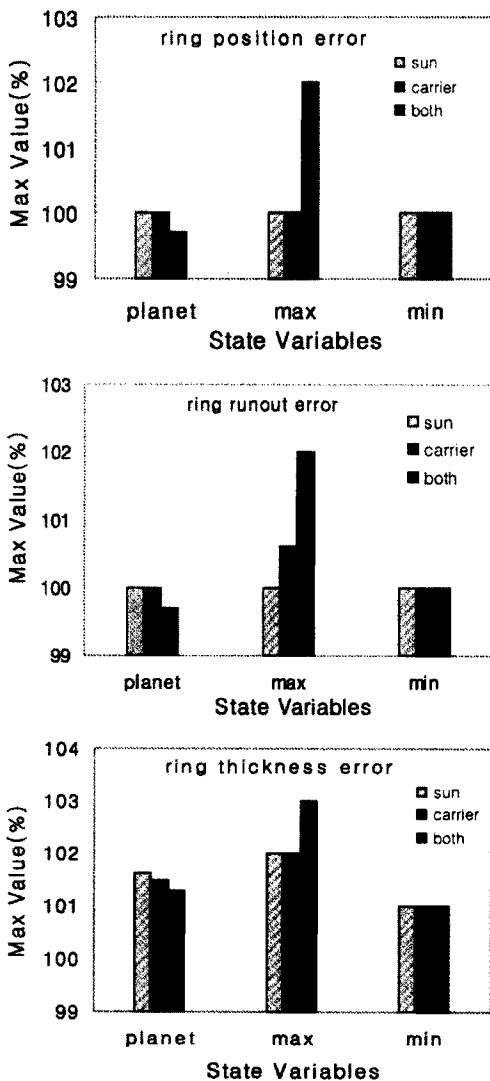


Fig. 13 Maximum percent value of planet bearing force, and maximum and minimum critical stresses as effects of a floating sun only, floating carrier only, and both, in ring gear error conditions

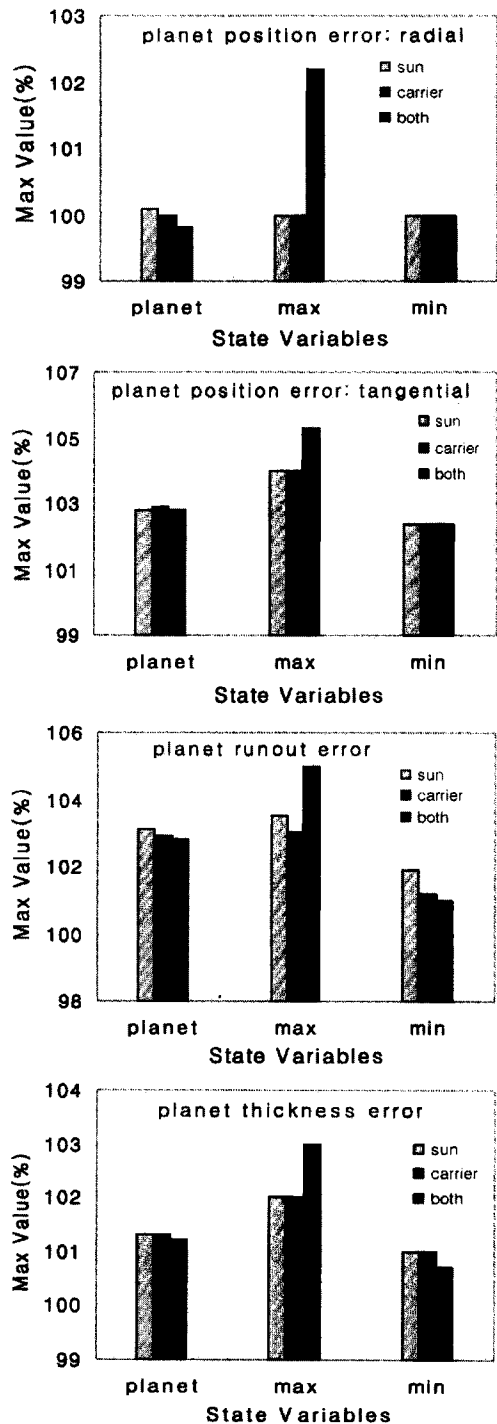


Fig. 14 Maximum percent value of planet bearing force, and maximum and minimum critical stresses as effects of a floating sun only, floating carrier only, and both, in planet error conditions

4. Conclusions

Hybrid finite element analysis was used to analyze the influence of bearing stiffness on the static properties of a planetary gear system with various manufacturing errors.

The effects of changes in stiffness were dominant in manufacturing error conditions than in no-error normal condition. However, the effects of changes in stiffness were similar for most of the manufacturing error conditions.

The state variables were affected most by planet bearing stiffness.

Floating either the sun or the carrier effectively equalizes load sharing and minimizes critical tooth stress. The effects of floating either the sun or the carrier are similar; however, floating both is not recommended because it can induce higher critical tooth stress. Planet bearing stiffness should be optimized by considering both bearing forces and critical stresses.

Acknowledgment

This paper was supported by Wonkwang University in 2004. We also acknowledge Dr. S. Vijayakar of Advanced Numerical Solutions, Inc. for his guidance and for making available the gear analysis program Planetary2D.

References

- ANSol, 2003, "Planetary2D User's Manual," Advanced Numerical Solutions.
- Bodas, A. and Kahraman, A., 2001, "Influence of Carrier and Gear Manufacturing Errors on the static Planet Load Sharing Behavior of Planetary Gear Sets," *Proc. JSME Int. Conf. on Motion and Power Transmissions*, MPT2001-Fukuoka, pp. 633~638.
- Cheon, G. J., Lee, D. H., Ryu, H. T., Kim, J. H. and Han, D. C., 1999, "A Study on the Dynamic Characteristics of an Epicyclic Gear Train with Journal Bearing," *SAE 1999-01-1052*.
- Cheon Gill-Jeong, Oh Jae-Kook, 2003, "Influence of Manufacturing and Assembly Errors on the Static Characteristics of Epicyclic Gear Trains," *Transactions of the KSME*, A, Vol. 27, No. 9, pp. 1597~1606.
- Cheon Gill-Jeong, 2003, "Influence of Ring Gear Boundary Conditions on the Static Characteristics of Epicyclic Gear Trains with Manufacturing Errors," *Transactions of the KSME*, A, Vol. 27, No. 11, pp. 1949~1957.
- Cheon Gill-Jeong, Parker, R. G., 2004, "Influence of Manufacturing Errors on the Dynamic Characteristics of Planetary Gear Systems," *KSME International Journal*, Vol. 18 No. 4, pp. 606~621.
- Hidaka, T. and Terauchi, Y., 1976, "Dynamic Behavior of Planetary Gear-1st Report, Load Distribution in Planetary Gear," *Bulletin of the JSME*, Vol. 19, pp. 690~698.
- James, B. and Harris, O., 2002, "Predicting Unequal Planetary Load Sharing Due to Manufacturing Errors and System Deflections, With Validation Against Test Data," *SAE 2002-01-0699*.
- Kahraman, A., 1994, "Planetary Gear Train Dynamics," *ASME J. of Mechanical Design*, Vol. 116, pp. 713~720.
- Kahraman, A. and Vijayakar, S., 2001, "Effect of Internal Gear Flexibility on the Quasi-Static Behavior of a Planetary Gear Set," *ASME J. of Mechanical Design*, Vol. 123, pp. 408~415.
- Kahraman, A., Kharazi, A. A. and Umrani, M., 2003, "A Deformable Body Dynamic Analysis of Planetary Gears with Thin Rims," *J. of Sound and Vibration*, 262, pp. 752~768.
- Lin, J. and Parker, R. G., 1999, "Analytical Characterization of the Unique Properties of Planetary Gear Free Vibration," *ASME J. of Vibration and Acoustics*, Vol. 121, pp. 316~321.
- Parker, R. G., Agashe, V. and Vijayakar, S. M., 2000, "Dynamic Response of a Planetary Gear System Using a Finite Element/Contact Mechanics Model," *ASME J. of Mechanical Design*, Vol. 122, pp. 304~310.
- Townsend, D. P., 1991, "Dudley's Gear Handbook," McGraw Hill.
- Vijayakar, S., 1991, "A Combined Surface Integral and Finite Element Solution for a Three-Dimensional Contact Problem," *Int. J. of Numerical Methods Eng.*, Vol. 31, pp. 525~545.